AnkyrinG is required to maintain axo-dendritic polarity in vivo

Jürgen-Markus Sobotzik[a,1], Jana Maria Sie[a], Chrisoula Politi[a], Domenico Del Turco[a], Vann Bennett[b], Thomas Deller[a], and Christian Schultz[a,1,2]

[a]Institute of Clinical Neuroanatomy, Neuroscience Center, Goethe-University, D-60590 Frankfurt/Main, Germany; and [b]Howard Hughes Medical Institute and Department of Cell Biology, Duke University Medical Center, Durham, NC 27710

Communicated by Peter C. Agre, Johns Hopkins Malaria Research Institute, Baltimore, MD, August 24, 2009 (received for review April 1, 2009)

Neurons are highly polarized cells that extend a single axon and several dendrites. Studies with cultured neurons indicate that the proximal portion of the axon, denoted as the axon initial segment (AIS), maintains neuronal polarity in vitro. The membrane-adaptor protein ankyrinG (ankG) is an essential component of the AIS. To determine the relevance of ankG for neuronal polarity in vivo, we studied mice with a cerebellum-specific ankG deficiency. Strikingly, ankG-depleted axons develop protrusions closely resembling dendritic spines. Such axonal spines are enriched with postsynaptic proteins, including ProSAP1/Shank2 and ionotropic and metabotropic glutamate receptors. In addition, immunofluorescence indicated that axonal spines are contacted by presynaptic glutamatergic boutons. For further analysis, double mutants were obtained by crossbreeding ankG$^{-/-}$ mice with L7/Purkinje cell-specific promoter 2 (PCP2) mice expressing enhanced green fluorescent protein (EGFP) in Purkinje cells (PCs). This approach allowed precise confocal microscopic mapping of EGFP-positive spiny axons and their subsequent identification at the electron microscopic level. Ultrastructurally, axonal spines contained a typical postsynaptic density and established asymmetric excitatory synapses with presynaptic boutons containing synaptic vesicles. In the shaft of spiny axons, typical ultrastructural features of the AIS, including the membrane-associated dense undercoating and cytoplasmic bundles of microtubules, were absent. Finally, using time-lapse imaging of organotypic cerebellar slice cultures, we demonstrate that nonspiny PC axons of EGFP-positive/ankG$^{-/-}$ mice acquire a spiny phenotype within a time range of only 3 days. Collectively, these findings demonstrate that axons of ankG-deficient mice acquire hallmark features of dendrites. AnkG thus is important for maintaining appropriate axo-dendritic polarity in vivo.

axon initial segment | axonal differentiation | diffusion barrier | cytoskeleton

Understanding the mechanisms of cellular polarization into distinct compartments is a fundamental issue in cell biology. Among all cell types with a complex morphology, neurons are characterized by exceptionally pronounced structural and functional segregation of distinct cell domains. The most fundamental level of neuronal polarity is represented by the establishment of axonal and somatodendritic domains (1, 2). Appropriate maintenance of these domains—specialized for either receiving (dendrites) or transmitting electrical signals (axons)—provides the underpinning for all neural circuitry (3). Structurally, dendrites and axons can be distinguished by their morphological appearance and their specific complements of organelles and cytoskeleton proteins. In addition, distinct sets of membrane proteins are enriched in either the somatodendritic or the axonal domain (3).

The structural and functional segregation of axons and dendrites—referred to as axo-dendritic polarity—is established early on in development (4, 5). Subsequently, axo-dendritic polarity must be maintained over the entire life span of the neuron. A unique axonal subdomain implicated in this process is the axon initial segment (AIS), which extends from the axon hillock to the beginning of the myelin sheath (6). The AIS serves not only as the initial generator but also as an important modulator of action potentials (7, 8). Moreover, a membrane-associated diffusion barrier is established in the AIS (9, 10). This barrier is based on a high density of transmembrane proteins recruited to the AIS by the membrane adaptor protein ankyrinG (ankG) (11, 12). AnkG indeed serves as the master organizer molecule of the AIS because other proteins, such as βIV spectrin and KCNQ2/3 channels, require ankG to appropriately cluster in the AIS (12–14).

Previously, a role of the AIS for maintaining segregation of axonal and somatodendritic membrane proteins was postulated (9, 10). Interestingly, a shift of dendritic features into proximal axons was indeed found in cultured hippocampal neurons treated with ankG short hairpin RNA (15). This observation provides direct evidence for a role of ankG in maintaining axo-dendritic polarity in vitro. In contrast, the potential relevance of ankG for neuronal polarization in vivo still remains undetermined. To address this issue, we examined mice with a cerebellum-specific deficiency for ankG (16). These mice lack the 270/480-kDa isoforms of ankG and are affected by ataxia, Purkinje cell loss, impaired firing of action potentials, and impaired AIS-specific localization of voltage-gated sodium channels. AISs of ankG-deficient Purkinje neurons also lack β-IV spectrin (13) and KCNQ2/3 channels (14). Moreover, 186-kDa neurofascin is not concentrated normally at ankG-deficient AISs (13) and formation of neurofascin-dependent axo-axonic synapses with interneurons is impaired (17).

In the present study, we document a profound structural reorganization of ankG-deficient Purkinje cell axons in vivo and show that they exhibit features normally associated with dendrites. These results indicate that ankG plays a central role in maintaining appropriate axo-dendritic polarity in vivo.

Results

The morphology of Purkinje cells (PCs) in ankG$^{-/-}$ mice was compared to that of wild-type animals, using immunofluorescent labeling of calbindin D28K, a calcium-binding protein enriched in PCs (Fig. 1*A*). Some principal features of PC polarity were found to be preserved in ankG$^{-/-}$ mice. Thus, a single axon emerged from the basal cell pole whereas dendrites originated from the opposite cell pole. AnkG$^{-/-}$ PC axons had a normal trajectory through the granule cell layer, fasciculating with other axons in the white matter. Accordingly, ankG deficiency appar-

Author contributions: J.-M.S. and C.S. designed research; J.-M.S., J.M.S., and C.P. performed research; D.D.T., V.B., and T.D. contributed new reagents/analytic tools; J.-M.S., J.M.S., D.D.T., T.D., and C.S. analyzed data; and C.S. wrote the paper.

The authors declare no conflict of interest.

[1]Present address: Electron Microscopy Unit, Institute for Anatomy and Cell Biology, Justus-Liebig-University, Aulweg 132, D-35385 Giessen, Germany.

[2]To whom correspondence should be addressed. E-mail: christian.schultz@anatomie.med.uni-giessen.de.

This article contains supporting information online at www.pnas.org/cgi/content/full/0909267106/DCSupplemental.

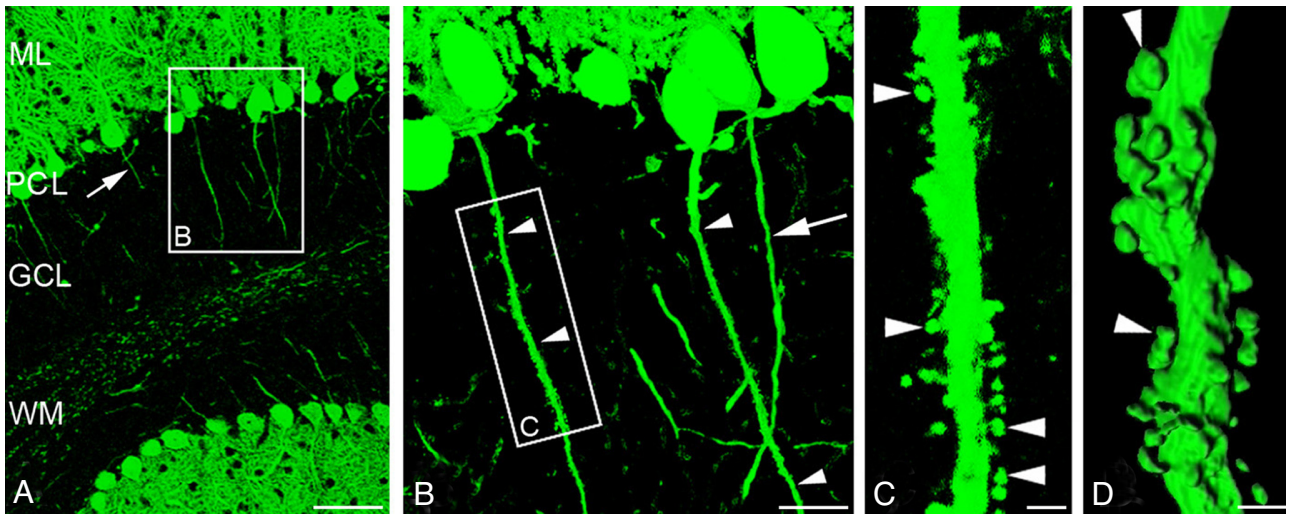

Fig. 1. AnkG-deficiency causes PC axons to develop spines in vivo. (*A–C*) The morphology of PC in ankG$^{-/-}$ mice is visualized by anti-calbindin D28K labeling. (*A*) At low magnification, principal features of axo-dendritic polarity are preserved. PC dendrites branch in the molecular layer (ML), PC somata are aligned in the Purkinje cell layer (PCL), and PC axons (arrow) traverse the granule cell layer (GCL) en route to the white matter (WM). (*B*) Higher magnification of framed area in *A*. Three PC axons originating from their parental cell body are depicted. Two of them (arrowheads) exhibit a conspicuous spiny appearance. By comparison, the third axon (arrow) shows a smooth surface. (*C*) Close-up view of framed area in *B*. The PC axon gives rise to numerous spiny protrusions. These spines have a thread-like neck and a mushroom-like head (arrowheads) and thus resemble dendritic spines. (*D*) The 3-dimensional morphology of a spiny PC axon is visualized by surface rendering of a confocal Z-stack. (Scale bars: *A*, 100 μm; *B*, 20 μm; *C* and *D*, 2 μm.)

ently does not interfere either with initial specification of PC axons or with axonal pathfinding in vivo.

Closer microscopic examination, however, revealed surprising morphological changes in PCs of ankG$^{-/-}$ mice. A substantial number of proximal axonal segments of PCs gave rise to cytoplasmic protrusions closely resembling dendritic spines (Fig. 1 *B–D*). The distribution and prevalence of spiny axons was studied in parasagittal sections of the cerebellar vermis [supporting information (*SI*) Fig. S1]. The highest prevalence was noted in the cerebellar nodule where 45% of all examined axons exhibited a spiny phenotype. By contrast, spiny axons were completely absent in ankG$^{+/+}$ mice. Spines were only rarely associated with the ankG-depleted AIS itself, but were mainly found along adjacent axonal segments. Spiny segments acquired a length of up to 160 μm, which is almost an order of magnitude longer than the AIS of a typical PC (18). Spiny axons had a considerably larger diameter as compared to nonspiny axons of ankG$^{-/-}$ mice (1.84 $\pm$ 0.33 μm vs. 0.93 $\pm$ 0.17 μm). During their transit through the granule cell layer, the thickened spiny axons tapered down into normal-sized nonspiny axons. The morphology of axonal spines was further analyzed by 3-dimensional surface rendering of confocal Z-stacks (Fig. 1*D*). Axonal spines typically had a mushroom-like appearance with a bulbous head connected to the shaft of the parent process via a thin neck. This morphology closely resembles dendritic PC spines. The spiny phenotype of PC axons in ankG$^{-/-}$ mice suggests that ankG contributes to proper segregation of the axonal and the somatodendritic domain in vivo. Our findings confirm and extend the recent in vitro data of Hedstrom et al. (15).

Dendritic spines represent neuronal microcompartments equipped with a multitude of cytoskeleton proteins, signaling complexes, and membrane-associated proteins (19). The concentration of actin filaments, for example, is strikingly high in dendritic spines as compared to other neuronal compartments (20). We detected filamentous actin in spiny axons using fluorescent phalloidin. The neck of aberrant axonal spines in ankG-depleted PCs was highly enriched with F-actin (Fig. 2 *A–C*), similar to the distribution of filamentous actin in dendritic spines. Dynamic modulation of the actin cytoskeleton by actin-binding proteins plays an important role in regulating spine morphology and synaptic plasticity (21). One of these actin-binding proteins is spinophilin/neurabin-II, which modulates excitatory synaptic transmission by recruiting protein phosphatase-1 to spines (22). Spinophilin accumulated in axonal spines of ankG$^{-/-}$ PC axons (Fig. 2 *D–F*), indicating that actin-associated proteins normally targeted to dendritic spines are shifted into the axonal compartment of ankG$^{-/-}$ PCs. Spinophilin was absent in nonspiny axons of ankG$^{-/-}$ mice and in ankG$^{+/+}$ PC axons.

In addition to detecting the aberrant shift of dendritic proteins into spiny axons (detailed above), we also examined the compartmentalization of the axon-specific protein tau (Fig. S2). Accumulation of tau was markedly reduced in spiny segments of ankG$^{-/-}$ mice as compared to nonspiny axons of control animals.

Dendritic spines serve as postsynaptic compartments for excitatory glutamatergic neurotransmission. This function is intimately connected with the postsynaptic density (PSD), a huge macromolecular complex consisting of several hundred different proteins (23, 24). We examined whether key components of the PSD are also enriched in axonal spines. We focused on proteins of the ProSAP/Shank family, which function as "master scaffolding proteins" of the PSD by binding simultaneously to glutamate receptor complexes and the postsynaptic cytoskeleton of the spine (25–27). First, we confirmed the previously reported somatodendritic clustering of ProSAP1/Shank2. In ankG$^{-/-}$ mice, however, small punctate structures intensively immunopositive for ProSAP1/Shank2 were specifically located in axonal spine heads (Fig. 2 *G–I*). Thus, lack of ankG causes important backbone proteins of the PSD to be specifically targeted to axonal spines.

The membrane of PC spines contains metabotropic and ionotropic glutamate receptors (GluRs). Thus, we tested whether postsynaptic GluRs are also present in axonal spines of ankG$^{-/-}$ PCs. First, the distribution of the postsynaptic metabotropic glutamate receptor 1 (mGluR1) was examined. In ankG$^{+/+}$ animals mGluR1 labeling was restricted to the somatodendritic domain as previously reported (28). In ankG$^{-/-}$ animals, however, mGluR1 labeling was found in the granule cell

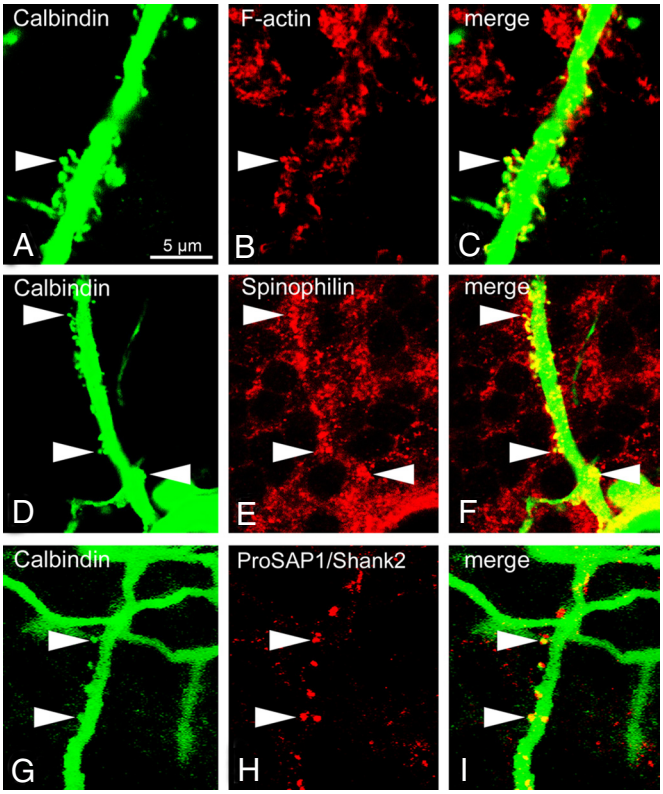

Fig. 2. Spiny PC axons of ankG$^{-/-}$ mice possess neurochemical features of axons and dendrites. (*A–C*) Enrichment of filamentous actin in spines of an ankG$^{-/-}$ PC axon (arrowhead). F-actin was labeled by fluorescent phalloidin. (*D–F*) Enrichment of the dendrite-specific protein spinophilin in spines of an ankG$^{-/-}$ PC axon (arrowheads). (*G–I*) Highly selective enrichment of the PSD protein ProSAP1/Shank2 in spines of an ankG$^{-/-}$ PC axon (arrowheads). (Scale bar, 5 μm.)

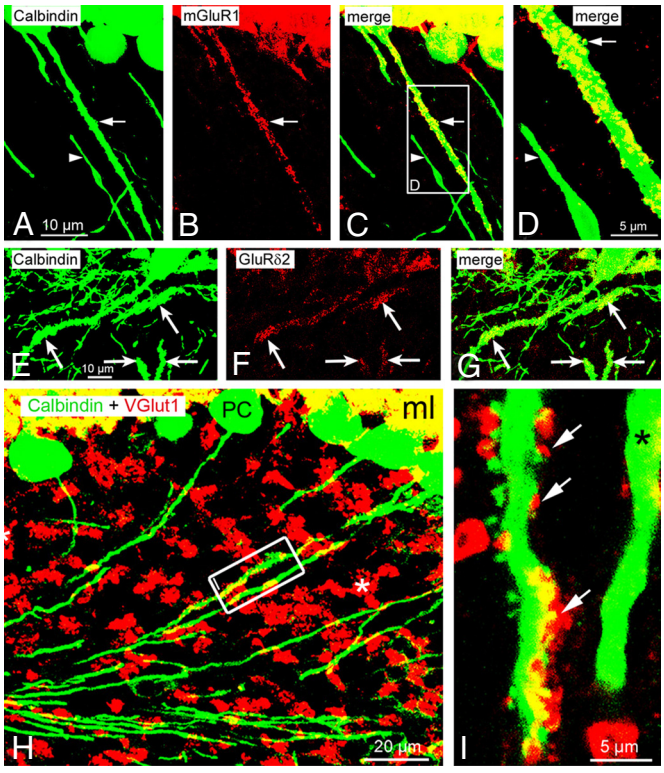

Fig. 3. Features of glutamatergic synapses associated with spines of ankG$^{-/-}$ PC axons. (*A–C*) Clustering of postsynaptic mGluR1 in a spiny PC axon (arrow). By comparison, a neighboring nonspiny PC axon (arrowhead) is completely devoid of mGluR1. (*D*) Close-up view of the framed area shown in *C*. Arrow points to a spine enriched with mGluR1. Arrowhead: nonspiny PC axon devoid of mGluR1. (*E–G*) Enrichment of postsynaptic GluRδ2 in spiny PC axons (arrows). Nonspiny axons beneath the PC layer belong to the plexus of PC axon collaterals. (*H* and *I*) Double labeling for calbindin D28K and VGlut1. (*H*) Asterisk denotes glutamatergic mossy fiber boutons associated with cerebellar glomeruli. Two PC axons in the framed area are shown at higher magnification in *I*. (*I*) Spines of a PC axon are contacted by VGlut1-positive boutons (arrows). A neighboring nonspiny axon (asterisk) is devoid of VGlut1-positive terminals.

layer, where it was associated with spiny PC axons (Fig. 3 *A–D*). Nonspiny PC axons were devoid of mGluR1 (Fig. 3 *A–D*, arrowheads). Next, we examined the distribution of GluRδ2, which specifically localizes to parallel fiber (PF)/Purkinje cell synapses (29). Again, an aberrant shift of GluRδ2 into spiny PC axons was found, whereas nonspiny axons of ankG$^{-/-}$ PCs were GluRδ2 negative (Fig. 3 *E–G*). These observations demonstrate that lack of ankG permits GluRs to enter the axonal domain.

Dendritic spines normally are contacted by glutamatergic axonal endings. We tested whether this is also the case for axonal spines of ankG$^{-/-}$ mice. The vesicular glutamate transporter 1 (VGlut1) was used as a marker for glutamatergic boutons (30). As shown in Fig. 3*H*, I spiny axons were indeed contacted by glutamatergic boutons (see also Fig. S3 *A–C*). Further confirmation for axonal boutons impinging on the axonal spines was obtained by double labeling against synaptophysin, a marker for presynaptic endings (Fig. S3 *D–F*). These observations indicate that axonal spines of ankG$^{-/-}$ mice serve as postsynaptic partners for presynaptic glutamatergic terminals.

Further insights into structural changes of ankG-depleted axons required the use of electron microscopy (EM). However, spiny axons were very difficult to identify by conventional techniques such as immunogold labeling. We circumvented this limitation by crossbreeding ankG$^{-/-}$ mice with mice that express enhanced green fluorescent protein (EGFP) under the control of the PC-specific promoter L7 (31). The PC somata of these double mutants gave rise to EGFP-positive spiny axons indistinguishable from those identified in ankG$^{-/-}$ single mutants. This allowed us to perform correlated light and electron microscopy (Fig. S4). As a first step, precise mapping of EGFP-positive spiny axons was achieved by confocal laser scanning microscopy (Fig. S4*A*). Subsequently, this topographic information served to identify spiny axons in ultrathin sections (Fig. S4 *B* and *C*). Spines of ankG-depleted axons were found to be contacted by terminal presynaptic boutons filled with synaptic vesicles (Fig. 4 *A–D*). Importantly, the axonal spine contained a thickened postsynaptic density (Fig. 4 *B* and *D*)—a hallmark for asymmetric and excitatory glutamatergic synapses. Together with our immunohistochemical findings these results confirm the aberrant postsynaptic nature of ankG-depleted spiny axons.

In serial ultrathin sections, the spiny axon illustrated in Fig. 4 could be traced over a distance of ≈80 μm extending from the PC soma into the granule cell layer. Interestingly, over this entire length the spiny axon was completely devoid of a myelin sheath (see also Fig. S4). By contrast, the first unmyelinated portion of the PC axon (corresponding to the length of the AIS) normally accounts only for the first 17 μm of the axon (18). Further confirmation for impaired myelination of spiny axons in ankG-depleted mice was obtained by immunofluorescent labeling of myelin basic protein—a major component of the myelin sheath (Fig. S5). Taken together, these data suggest that lack of ankG interferes with proper myelination of proximal axonal segments.

At the ultrastructural level, the AIS can be distinguished by 2 features: (*i*) an electron-dense undercoating beneath the cyto-

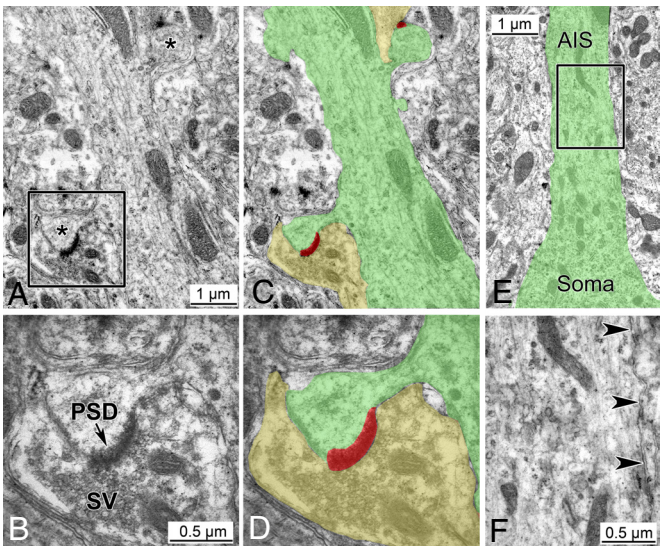

Fig. 4. Ultrastructural features of spiny axons in L7-EGFP/ankG$^{-/-}$ double mutants. (*A* and *C*) The shaft of an ankG-depleted axon gives rise to mushroom-like spines (asterisks in *A*). Shades of color in *C* delineate the contour of a spiny axon (green) and 2 associated presynaptic terminals (yellow). PSDs associated with the axonal spines are shaded in red. See Fig. S3 for confocal scanning microscopy of the same spiny axon. (*B* and *D*) Close-up view of the framed area in *A*. The spine of the ankG-depleted axon is endowed with a PSD and contacted by a presynaptic terminal containing numerous synaptic vesicles (SV). Colors in *D* correspond to those in *C*. (*E* and *F*) Ultrastructure of the ankG-depleted AIS. *E* depicts the transition of a PC soma into the AIS of the spiny axon also shown in *A*–*D* (contour delineated by green color). (*F*) Close-up view of the framed area in *E*. The cytoplasmic membrane of the ankG-depleted AIS (arrowheads) lacks the dense undercoating normally found in the AIS. Likewise, the AIS cytoplasm is devoid of fasciculated microtubules. For comparison with an AIS of a control animal see Fig. S6.

plasmic membrane and (*ii*) fascicles of cytoplasmic microtubules (32). Of note, both of these ultrastructural AIS features were absent in proximal segments of spiny PC axons (Fig. 4 *E* and *F*). In contrast, these features were present in AISs of control animals (Fig. S6). Thus the acquisition of dendritic features by ankG-deficient axons is accompanied by a loss of AIS-specific ultrastructural features.

The development of spiny axons was further examined using organotypic cerebellar slice cultures prepared from L7-EGFP/ankG$^{-/-}$ double mutants at P9–P10. Confocal time-lapse imaging revealed the spiny morphology of EGFP-positive PC axons (Fig. 5 *A*–*C*). The altered axons exhibited all of the dendritic features detailed above (summarized in Fig. S7). A subset of EGFP-positive PC axons was mapped and confocal Z-stacks of identified axons were acquired every other day. This approach allowed us to detect the conversion of nonspiny into spiny axons over a time range of only 3 days (Fig. 5 *D*–*I*). Such acquisition of a spiny phenotype consistently was accompanied by a thickening of the converting axon. Spiny axons were stable over the entire period of observation. Thus, a conversion of a spiny into a nonspiny phenotype was not observed. This supports the notion that ankG depletion does not interfere with early axon specification but rather with long-term maintenance of axonal identity.

Discussion

This study documents a profound dendritic reorganization of ankG-depleted axons in vivo. Core components of the somatodendritic compartment were found to be shifted into the axonal compartment of ankG-deficient neurons. This shift was accompanied by outgrowth of cytoplasmic axonal protrusions closely resembling dendritic spines. Time-lapse imaging of EGFP-expressing ankG-depleted PC axons demonstrated a conversion of inconspicuous nonspiny axons into spiny axons over a time range of only 3 days. Most notably, aberrant axonal spines were equipped with postsynaptic glutamate receptors and served as contact sites for presynaptic glutamatergic boutons as revealed by electron microscopic analysis. Thus, depletion of ankG interferes with the maintenance of axonal identity by imposing hallmark features of postsynaptic dendrites on axons in vivo.

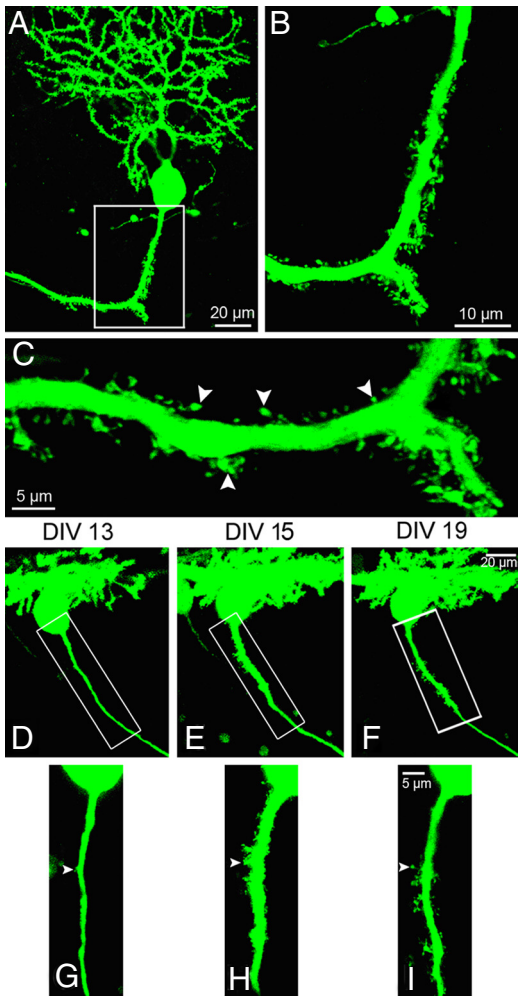

Fig. 5. Identification and time-lapse imaging of spiny axons in cerebellar slice cultures prepared from L7-EGFP/ankG$^{-/-}$ mice. (*A*–*C*) EGFP-positive spiny PC axon identified in a cerebellar slice culture (DIV10) of an L7-EGFP/ankG$^{-/-}$ mouse. The spiny appearance of this process (arrowheads) closely resembles that of axons found in cerebellar brain sections of ankG$^{-/-}$ mice (see Fig. 1). (*D*–*I*) Confocal time-lapse imaging of a cerebellar slice culture reveals the conversion of a nonspiny into a spiny axon. At DIV13, the selected axon is largely devoid of spines except for a single protrusion (arrowhead). Between DIV13 (*D*) and DIV15 (*E*) the conversion into a spiny axon occurs. This conversion into an axo-dendritic hybrid is accompanied by an enlargement of the axonal diameter. (Scale bars: *A* and *D*–*F*, 20 μm; *B*, 10 μm; *C* and *G*–*I*, 5 μm.)

Development of spines and associated glutamatergic synapses is a highly complex process that requires appropriate trafficking, assembly, and coordinated interaction of a multitude of regulatory proteins (19). What are the key molecules responsible for aberrant spinogenesis and glutamatergic synaptogenesis associated with ankG-depleted axons? Two major candidate proteins include the PSD-associated protein ProSAP/Shank and the glutamate receptor GluRδ2. With regard to ProSAP/Shank, a central role of this molecule for spinogenesis was previously proposed on the basis of

the following findings: (*a*) ProSAP/Shank is an early component of the PSD during synaptogenesis (33), (*b*) overexpression of ProSAP/Shank induces enlargement of dendritic spine heads (34), and (*c*) transfection of ProSAP/Shank induces spine formation in dendrites of cerebellar granule cells that are normally nonspiny (35). Moreover, these spines are contacted by functional glutamatergic synapses. Accordingly, ProSAP/Shank recruits the necessary cytoskeletal and membrane components that enable the postsynaptic membrane of dendrites to reorganize into a spine-like structure involved in glutamatergic neurotransmission. It is thus conceivable that a shift of ProSAP1/Shank2 into proximal ankG$^{-/-}$ axons may play an important role in aberrant axonal spinogenesis.

With regard to GluRδ2, it is known that this receptor plays a major role in recruitment of glutamatergic presynaptic terminals to postsynaptic PC spines in vivo (29, 36). Heterologous expression of GluRδ2 in HEK cells cocultured with cerebellar granule cells attracts presynaptic glutamatergic terminals even to the nonneuronal HEK cells (36). Thus, on the basis of its well-established role as a presynaptic organizer, we suggest that GluRδ2—together with ProSAP/Shank—may play a key role in driving glutamatergic synaptogenesis associated with aberrant spines of ankG-depleted axons.

Previous in vitro studies pointed out that depletion of ankG could compromise the AIS-specific membrane diffusion barrier (2, 9, 10) and thus abolish segregation of somatodendritic vs. axonal membrane proteins (15). However, this mechanism alone cannot explain the highly complex restructuring that must underlie the conversion of a normal axon into a spiny axo-dendritic hybrid. The question therefore has to be raised whether additional functions of ankG in the AIS may contribute to maintaining neuronal polarity. In this regard, previous studies on epithelial cells may provide valuable clues linking ankG to even more profound mechanisms of membrane metabolism. In epithelial cells, ankG is associated with the lateral membrane (37). Interestingly, RNAi-induced depletion of ankG in epithelial cells caused a dramatic loss of the lateral membrane whereas apical and basal membrane domains expanded (37, 38). In addition to simply modifying the biophysical characteristics of a given membrane domain, ankG thus is also responsible for entire membrane biogenesis (38). It will be of interest to determine whether ankG exerts a similar function in the AIS. Impaired biogenesis of the entire AIS membrane would offer an alternative explanation for the profound morphological changes of ankG-depleted axons.

Of note, the aberrant shift of dendritic components into ankG-depleted axons not only was restricted to membrane-associated proteins (such as GluRs) but also included cytoplasmic proteins such as the actin-regulating protein spinophilin. This shift of cytoplasmic components can hardly be attributed to an impaired membrane diffusion barrier. Indeed, a recent study provides direct evidence for an ankG-dependent cytoplasmic filter in the AIS (39). This cytoplasmic AIS filter controls the diffusion of macromolecules and transport of vesicular carriers into the axon and is perturbed by depletion of ankG (39). Thus a combined disruption of both membrane-associated and cytoplasmic filtering in the AIS may underlie the dendritic reorganization of axons in ankG-depleted mice. This notion is confirmed and extended by our current electron microscopic analysis demonstrating absence not only of the membrane-associated dense undercoating but also of cytoplasmic microtubule bundles in ankG-depleted spiny axons. This analysis suggests that ankG couples the function and integrity of the membrane cytoskeleton to that of the cytoplasmic microtubule system of the AIS. Interestingly, the AIS-specific 480-kDa isoform of ankG with its highly elongated tail domain (length $\approx$0.5 μm) (11) is an ideal candidate to connect microtubules to spectrin-associated actin filaments (40). Moreover, the fasciculated microtubules of the AIS are known to provide important directional cues for anterograde axonal transport (41). Disrupting the microtubule architecture of the AIS may thus contribute to the partial loss of the axonal phenotype documented in the present study. Unraveling the precise molecular mechanisms that underlie these structural changes will help us to fully understand the crucial role of ankG for maintaining appropriate neuronal polarity in vivo.

Materials and Methods

Animals. Animals were raised and housed under standard laboratory conditions. All animal experiments were performed in compliance with German law on the use of laboratory animals. For time-lapse imaging of cerebellar slice cultures, ankG$^{-/-}$ mice were crossbred with L7/Purkinje cell-specific promoter 2 (PCP2)-EGFP transgenic mice expressing EGFP under the direction of a Purkinje cell-specific promoter (L7/PCP2) (31). L7/PCP2-EGFP mice were purchased from Jackson Laboratory. AnkG and EGFP genotypes were determined as described (13, 16).

Antibodies. Antibodies against the ionotropic GlurR1 and GluRδ2, the mGluR1α, myelin basic protein, and synaptophysin were purchased from Chemicon International. A polyclonal antibody directed against residues 286–390 of spinophilin/neurabin-II was purchased from Upstate Cell Signaling Solutions. Polyclonal anti-ProSAP1/Shank2 (27) was kindly provided by Tobias Boeckers (Department of Anatomy and Cell Biology, University of Ulm, Ulm, Germany). Polyclonal antibodies against anti-calbindin D28K were purchased from Swant. Alexa 568 phalloidin was purchased from MoBiTec GmbH. VGlut1 was purchased from Synaptic Systems GmbH. The monoclonal antibody AT270 (Pierce Scientific, 1:1,000) was used to detect the axonal protein tau. All primary antibodies were used at a dilution of 1:500.

Immunohistochemistry. Adult mice were anesthetized with pentobarbital and transcardially perfused with 4% paraformaldehyde (PFA) in PBS, pH 7.4. Brains were removed and fixed in 4% PFA in PBS overnight. Sagittal vibratome sections (thickness 50 μm) were incubated with primary antibodies for 24 h at room temperature (RT). Bound antigens were detected by secondary antibodies conjugated with Alexa Fluor 488 or Alexa Fluor 568 (1:1,000; Molecular Probes).

Confocal Laser Scanning Microscopy. For confocal microscopy, a laser scanning microscope (LSM 510, Carl Zeiss) was used. Optical reconstruction of confocal Z-stacks was performed using the implemented LSM5 software. Three-dimensional surface renderings were generated using the Imaris software package (Bitplane AG). Photoshop CS2 (Adobe Systems) was used to optimize contrast and brightness. Detector gain and amplifier offset was set to obtain pixel densities within the linear range. AIS fluorescence intensity was measured using implemented functions of the LSM 510 (Carl Zeiss MicroImaging).

Electron Microscopy. For electron microscopy, mice were transcardially perfused with 0.9% NaCl followed by perfusion with 4% paraformaldehyde and 0.5% glutaraldehyde. Serial sagittal sections (50 μm) of the cerebellar vermis were cut using a Vibratome (VT1000S, Leica). TO-PRO-3 (Molecular Probes, 1:5,000 in 1$\times$ PBS) was used for fluorescent counterstaining of cell nuclei. Sections were mounted on slides and coverslipped using aqueous fluorescence mounting medium. Subsequently, precise mapping of EGFP-positive spiny axons and surrounding TO-PRO-3-labeled nuclei was performed by recording Z-stacks of laser confocal microscopy images (see Fig. S4). Sections were carefully removed from the slide and postfixed in 2.5% glutaraldehyde (24 h, RT). The Vibratome sections were treated with 1% OsO_4 before being dehydrated and flat-embedded in Epon. Serial ultrathin sections were placed on 100-mesh copper grids (Plano GmbH), stained with uranyl acetate and lead citrate, and analyzed using a Zeiss EM 902 equipped with a cooled CCD camera (TRS). Fig. S4 exemplifies the successful identification of a spiny axon in ultrathin sections by means of correlation with previous laser microscopic mapping of EGFP and TO-PRO-3.

Light Microscopic Mapping of the Distribution and Diameter of Spiny Axons. The distribution of spiny axons was mapped in calbindin-labeled sections of the cerebellar vermis. Only axons that could be traced from their parental PC soma for a distance of at least 50 μm were included. A total of 1,756 axons were mapped in ankG-depleted mice (n = 3) and compared to 1,378 axons of ankG$^{+/+}$ (n = 3) animals. The percentage of spiny axons was calculated for each vermal lobule (I–X) separately. The diameter of PC axons was assessed at a distance of 40 μm from the PC axon hillock.

Organotypic Cerebellar Slice Cultures. Organotypic cerebellar slices were cultured according to a modified protocol (42). Slices were prepared at postnatal days 9 and 10. After decapitation, cerebelli were removed and sagittal sections were cut at 350 μm using a McIlwain mechanical tissue chopper (Science

Products). Slices were placed onto porous membranes (Millicell-CM, Millipore) and put into 6-well plates containing culture medium (50% minimum essential medium, 25% HBSS, 25% normal horse serum, 0.5% Glutamax, 4.2 mM glucose, 10 mM Hepes, and 0.5% sodium bicarbonate). The buffer was adjusted to pH 7.3. Cultures were incubated at 35 °C in a humidified atmosphere (5% CO_2). The medium was exchanged every other day.

Time-Lapse Imaging of Organotypic Cerebellar Slice Cultures. Time-lapse imaging was performed each day from days in vitro (DIV)9 to DIV21 with an upright Zeiss LSM PASCAL microscope. During imaging the culture medium was replaced with warm (35 °C) imaging buffer containing 129 mM NaCl, 4 mM KCl, 1 mM $MgCl_2$, 2 mM $CaCl_2$, 4.2 mM glucose, 10 mM Hepes, 0.1 mM Trolox, 0.1 mg/mL streptomycin, and 100 units/mL penicillin. The buffer was adjusted to pH 7.4 and to 365 mOsm/kg. A 10× water immersion objective (NA: 0.3) was used to locate identified axons. High-resolution images of identified axons were obtained using a 63× water immersion objective (NA: 0.95). Confocal Z-stacks were assessed at intervals of 0.5 μm.

ACKNOWLEDGMENTS. We thank Anke Biczysko, Ute Fertig, Heike Korff, Charlotte Nolte-Uhl, Gerd Magdowski, and Gerhard Kripp for technical assistance; Andreas Vlachos, M.D., and Ekaterina Copanaki, Ph.D., for help with time-lapse imaging; and Christian M. Müller, Ph.D., for helpful discussions. This work was supported by a grant from the Deutsche Forschungsgemeinschaft (Schu 1412/2- 1).

1. Craig AM, Banker G (1994) Neuronal polarity. *Annu Rev Neurosci* 17:267–310.
2. Winckler B, Mellman I (1999) Neuronal polarity: Controlling the sorting and diffusion of membrane components. *Neuron* 23:637–640.
3. Horton AC, Ehlers MD (2003) Neuronal polarity and trafficking. *Neuron* 40:277–295.
4. Arimura N, Kaibuchi K (2007) Neuronal polarity: From extracellular signals to intracellular mechanisms. *Nat Rev Neurosci* 8:194–205.
5. Barnes AP, Solecki D, Polleux F (2008) New insights into the molecular mechanisms specifying neuronal polarity in vivo. *Curr Opin Neurobiol* 18:44–52.
6. Ogawa Y, Rasband MN (2008) The functional organization and assembly of the axon initial segment. *Curr Opin Neurobiol* 18:307–313.
7. Kole MH, Letzkus JJ, Stuart GJ (2007) Axon initial segment Kv1 channels control axonal action potential waveform and synaptic efficacy. *Neuron* 55:633–647.
8. Bender KJ, Trussell LO (2009) Axon initial segment Ca2+ channels influence action potential generation and timing. *Neuron* 61:259–271.
9. Winckler B, Forscher P, Mellman I (1999) A diffusion barrier maintains distribution of membrane proteins in polarized neurons. *Nature* 397:698–701.
10. Nakada C, et al. (2003) Accumulation of anchored proteins forms membrane diffusion barriers during neuronal polarization. *Nat Cell Biol* 5:626–632.
11. Bennett V, Baines AJ (2001) Spectrin and ankyrin-based pathways: Metazoan inventions for integrating cells into tissues. *Physiol Rev* 81:1353–1392.
12. Yang Y, Ogawa Y, Hedstrom KL, Rasband MN (2007) betaIV spectrin is recruited to axon initial segments and nodes of Ranvier by ankyrinG. *J Cell Biol* 176:509–519.
13. Jenkins SM, Bennett V (2001) Ankyrin-G coordinates assembly of the spectrin-based membrane skeleton, voltage-gated sodium channels, and L1 CAMs at Purkinje neuron initial segments. *J Cell Biol* 155:739–746.
14. Pan Z, et al. (2006) A common ankyrin-G-based mechanism retains KCNQ and NaV channels at electrically active domains of the axon. *J Neurosci* 26:2599–2613.
15. Hedstrom KL, Ogawa Y, Rasband MN (2008) AnkyrinG is required for maintenance of the axon initial segment and neuronal polarity. *J Cell Biol* 183:635–640.
16. Zhou D, et al. (1998) AnkyrinG is required for clustering of voltage-gated Na channels at axon initial segments and for normal action potential firing. *J Cell Biol* 143:1295–1304.
17. Ango F, et al. (2004) Ankyrin-based subcellular gradient of neurofascin, an immunoglobulin family protein, directs GABAergic innervation at purkinje axon initial segment. *Cell* 119:257–272.
18. Somogyi P, Hamori J (1976) A quantitative electron microscopic study of the Purkinje cell axon initial segment. *Neuroscience* 1:361–365.
19. Calabrese B, Wilson MS, Halpain S (2006) Development and regulation of dendritic spine synapses. *Physiology (Bethesda)* 21:38–47.3.
20. Fifkova E (1985) Actin in the nervous system. *Brain Res* 356:187–215.
21. Carlisle HJ, Kennedy MB (2005) Spine architecture and synaptic plasticity. *Trends Neurosci* 28:182–187.
22. Allen PB, Ouimet CC, Greengard P (1997) Spinophilin, a novel protein phosphatase 1 binding protein localized to dendritic spines. *Proc Natl Acad Sci USA* 94:9956–9961.
23. Cheng D, et al. (2006) Relative and absolute quantification of postsynaptic density proteome isolated from rat forebrain and cerebellum. *Mol Cell Proteomics* 5:1158–1170.
24. Sheng M (2001) Molecular organization of the postsynaptic specialization. *Proc Natl Acad Sci USA* 98:7058–7061.
25. Naisbitt S, et al. (1999) Shank, a novel family of postsynaptic density proteins that binds to the NMDA receptor/PSD-95/GKAP complex and cortactin. *Neuron* 23:569–582.
26. Sheng M, Kim E (2000) The Shank family of scaffold proteins. *J Cell Sci* 113(Pt 11):1851–1856.
27. Boeckers TM, Bockmann J, Kreutz MR, Gundelfinger ED (2002) ProSAP/Shank proteins—a family of higher order organizing molecules of the postsynaptic density with an emerging role in human neurological disease. *J Neurochem* 81:903–910.
28. Das SS, Banker GA (2006) The role of protein interaction motifs in regulating the polarity and clustering of the metabotropic glutamate receptor mGluR1a. *J Neurosci* 26:8115–8125.
29. Hashimoto K, et al. (2001) Roles of glutamate receptor delta 2 subunit (GluRdelta 2) and metabotropic glutamate receptor subtype 1 (mGluR1) in climbing fiber synapse elimination during postnatal cerebellar development. *J Neurosci* 21:9701–9712.
30. Fremeau RT, Jr, Voglmaier S, Seal RP, Edwards RH (2004) VGLUTs define subsets of excitatory neurons and suggest novel roles for glutamate. *Trends Neurosci* 27:98–103.
31. Tomomura M, Rice DS, Morgan JI, Yuzaki M (2001) Purification of Purkinje cells by fluorescence-activated cell sorting from transgenic mice that express green fluorescent protein. *Eur J Neurosci* 14:57–63.
32. Peters A, Proskauer CC, Kaiserman-Abramof IR (1986) The small pyramidal neuron of the rat cerebral cortex. The axon hillock and the initial segment. *J Cell Biol* 39:604–619.
33. Petralia RS, Sans N, Wang YX, Wenthold RJ (2005) Ontogeny of postsynaptic density proteins at glutamatergic synapses. *Mol Cell Neurosci* 29:436–452.
34. Sala C, et al. (2001) Regulation of dendritic spine morphology and synaptic function by Shank and Homer. *Neuron* 31:115–130.
35. Roussignol G, et al. (2005) Shank expression is sufficient to induce functional dendritic spine synapses in aspiny neurons. *J Neurosci* 25:3560–3570.
36. Kakegawa W, et al. (2009) The N-terminal domain of GluD2 (GluRdelta2) recruits presynaptic terminals and regulates synaptogenesis in the cerebellum in vivo. *J Neurosci* 29:5738–5748.
37. Kizhatil K, Bennett V (2004) Lateral membrane biogenesis in human bronchial epithelial cells requires 190-kDa ankyrin-G. *J Biol Chem* 279:16706–16714.
38. Kizhatil K, et al. (2007) Ankyrin-G and beta2-spectrin collaborate in biogenesis of lateral membrane of human bronchial epithelial cells. *J Biol Chem* 282:2029–2037.
39. Song AH, et al. (2009) A selective filter for cytoplasmic transport at the axon initial segment. *Cell* 136:1148–1160.
40. Davis JQ, Bennett V (1984) Brain ankyrin. A membrane-associated protein with binding sites for spectrin, tubulin, and the cytoplasmic domain of the erythrocyte anion channel. *J Biol Chem* 259:13550–13559.
41. Nakata T, Hirokawa N (2003) Microtubules provide directional cues for polarized axonal transport through interaction with kinesin motor head. *J Cell Biol* 162:1045–1055.
42. Stoppini L, Buchs PA, Muller D (1991) A simple method for organotypic cultures of nervous tissue. *J Neurosci Methods* 37:173–182.